
Article:
Thermou, G.E. orcid.org/0000-0002-9569-0176, Katakalos, K. and Manos, G. (2018) Experimental investigation of substandard RC columns confined with SRG jackets under compression. Composite Structures, 184. pp. 56-65. ISSN 0263-8223

https://doi.org/10.1016/j.compstruct.2017.09.082

Experimental investigation of substandard RC columns confined with SRG jackets under compression

Georgia E. Thermou[1,2*], Konstantinos Katakalos[2], George Manos[2]

[1] Civil and Structural Engineering Department, The University of Sheffield, S1 3JD, Sheffield, UK

[2] Aristotle University of Thessaloniki, Dept. of Civil Engineering, 54124, Thessaloniki, Greece

Abstract: This paper aims to explore the behaviour of substandard reinforced concrete (RC) columns confined with Steel-Reinforced Grout (SRG) jackets under monotonically increasing uniaxial compression. A total of 24 specimens of short RC columns of square cross section were designed to fail due to longitudinal reinforcement buckling. Single-layered SRG jackets were applied to 18 of these specimens, whereas the rest served for control without SRG jackets. Parameters of this investigation were the type and density of the steel fabric as well as the corner radius of the cross section. The employed SRG jacketing managed to increase the strength and strain capacity and postpone the buckling of the longitudinal steel bars to occur at higher compressive strain level. Confinement effectiveness with respect to the lateral confining pressure exerted by the used SRG jacketing is discussed along with the observed mode of failure.

Keywords: Fabrics/textiles, Buckling, Fibre/matrix bond, Mechanical testing, Seismic strengthening

1. Introduction

Old-type reinforced concrete (RC) members are characterized by poor quality of materials and insufficient reinforcement detailing (Fig. 1(a-b)). Transverse reinforcement representative of the construction practice before the 1970's in South Europe comprises smooth bars with their ends simply overlapping at the corner, placed at large distance between them which may

* Corresponding author, tel: +44 (0) 114 222 5071, g.thermou@sheffield.ac.uk

increase further in case of stirrups rendered ineffective due to corrosion as shown in Fig. 1(c). Such a sparse arrangement of stirrups results in a large unsupported length of the longitudinal reinforcing bars, rendering them susceptible to buckling failure when subjected to a critical compressive load. The safe performance of the whole building could be jeopardized by localized damage in the plastic hinge regions of the columns, where sideways buckling of compression reinforcement is expected to occur due to lateral shear distortion of the member in that region (Fig. 1(d)).

Previous research has identified the key role of the ratio of stirrup spacing, s, to bar diameter, D_b, in the stability of compression reinforcing bars supported laterally by stirrups [e.g. 1-5]. The values of s/D_b could range between 6 and 8 in case of high to moderate ductility RC members [6]. For slenderness ratios higher than eight (s/Db>8), the compression reinforcing bars could reach buckling stage when their compressive stress reaches yielding point [5]. According to the detailing of the pre-1970's era, s/D_b could receive any value between 10 and 40 [7].

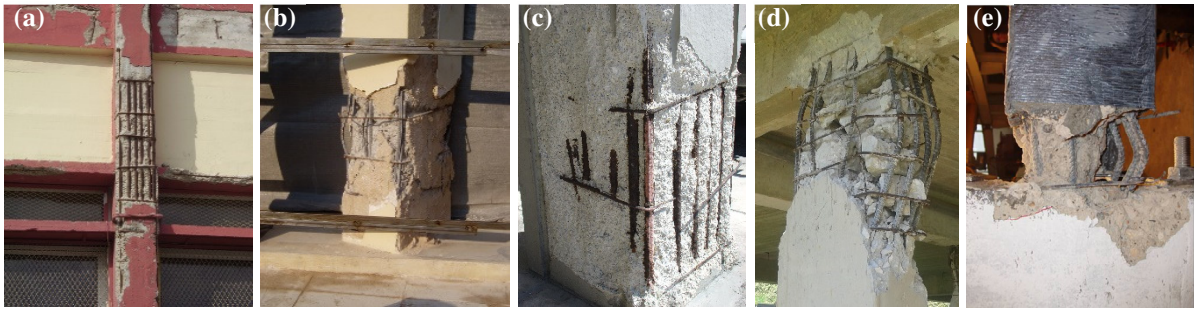

Figure 1: (a)-(c) Reinforcement detailing of RC columns built before the 1970's in South Europe; (d) Failure due to reinforcement buckling; (e) Buckling of longitudinal reinforcement in FRP-jacketed RC columns (source: personal files).

The beneficial effect on the compressive performance of substandard R/C columns, when CFRP jackets are used effectively as external confinement, was observed in the past [8, 9]. Moreover, composite systems with inorganic (e.g. FRPs) and organic binders (e.g. TRM) are efficient in preventing premature bar buckling and postponing it to higher ductility strain levels

[e.g. 7, 10, 11]. When the longitudinal reinforcement reaches conditions of instability at the critical axial strain, the bar bends laterally to maintain compatibility with the increasing axial strain of the supporting concrete core [3]. Wrapping with the composite fabrics allows the concrete in compression to increase its strain capacity. As long as the strain capacity of the confined concrete is higher than the critical strain at the onset of reinforcement buckling, the member will deform further up to the point where the stress concentrations will limit the effectiveness of the composite jacket as lateral support of the longitudinal reinforcement (Fig. 1(e)) [6]. In a recent study of Bournas and Triantafillou [12] the superior behaviour of TRM jackets compared to FRP jackets has been demonstrated. It has been observed that TRM jackets allow for higher local deformations as they are able to deform outward without early fiber rupture. Thus, during buckling, when longitudinal bars bend outward at the corners of the section, TRM jackets receive the developed stress concentrations without failure.

Steel-Reinforced Grout (SRG) jacketing is a relatively new composite system where high strength steel reinforced fabric is combined with cementitious grout [13]. Earlier studies conducted on SRG confined concrete under uniaxial compression have demonstrated the efficiency of the system in increasing strength and axial strain capacity [14-16]. In the present study, the effectiveness of SRG jacketed lightly reinforced RC columns was experimentally investigated. The specimens were designed as to be susceptible to rebar buckling failure with the compression reinforcing bars losing their stability prior or close to yielding. The ratio of stirrup spacing to longitudinal bar diameter was equal to 20. Alternative single-layered SRG jackets were applied to 18 square cross section columns, whereas 6 more were used as control specimens. Experimental evidence has shown that the single-layered SRG jackets increased strength and deformation capacity. The lateral confining pressure exerted by the jackets was sufficient to increase the compressive strain ductility, thus delaying bar buckling failure to occur at higher compressive strain level.

2. Experimental program

2.1 Test specimens and material properties

The experimental program comprised twenty-four RC column specimens representative of the construction practice before the 1970's in South Europe. These specimens had a 150 mm square cross section representing a 1:2 scaled model of a prototype column with a 300 mm square cross section. The height of the specimens was defined at 600 mm due to restriction imposed by the available loading frame. With the aspect ratio being equal to 4 (=h/b=600/150=4, where h is the height of the specimen, b is the width of the cross section) no stability problems were expected to occur [17,18].

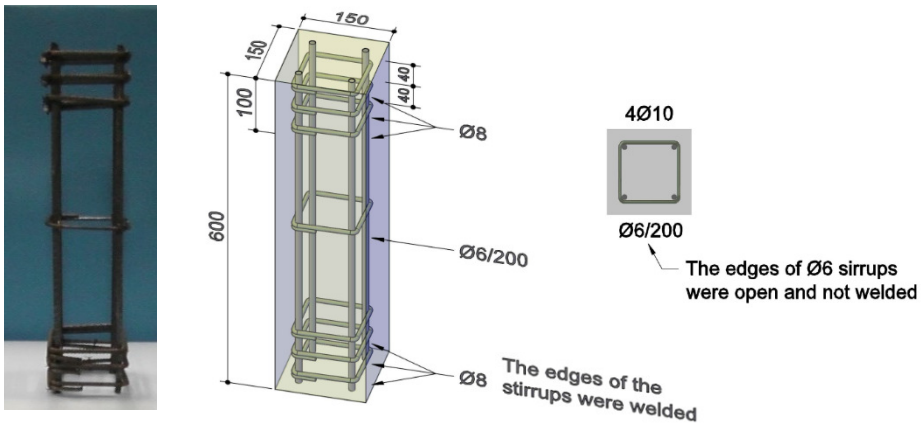

Figure 2: Geometry and reinforcement detailing of the columns (dimensions in mm).

The specimens, with a geometry in mm as shown in Fig. 2, featured a low percentage of longitudinal reinforcement and sparse transverse reinforcement, representative of old type detailing. Longitudinal reinforcement comprised four corner 10 mm diameter bars (4∅10, longitudinal reinforcement ratio, ρ_ℓ=1.4%) and 6 mm diameter stirrups with their ends bent at 90^0 spaced at s=200 mm (∅6/200). The s/D_b ratio was selected to be high (s/D_b=20) complying with old type detailing requirements of that era. As seen in Fig. 2, three additional 8 mm stirrups (tie ends were welded) were placed at the specimen ends near the loading surfaces, to prevent local cracking of concrete due to stress concentrations. The concrete cover was equal to 15 mm.

The twenty-four columns were divided into two groups based on whether the four corners of the square cross section were rounded off or not. Fifteen out of the twenty-four columns had their corners rounded off by a corner radius r=25 mm. Parameters of investigation were apart from the corner radius, the type (12X, 3X2) and the density of the fabric (1 cord/cm, 2 cords/cm) (Fig. 3). The geometrical and mechanical properties of a single cord 12X and 3X2 as measured in tests conducted are presented in Table 2 [15] and the average stress – strain curves appear in Fig. 4. The density was 1 cord/cm and 2 cords/cm corresponding to an equivalent thickness of 0.062 mm and 0.124 mm, respectively. The axial stiffness of the 1 cord/cm and 2 cords/cm steel fabric utilized herein is equal to about 1/3 and 2/3 of the axial stiffness of a common carbon fabric (≈25000 N/mm, Table 2).

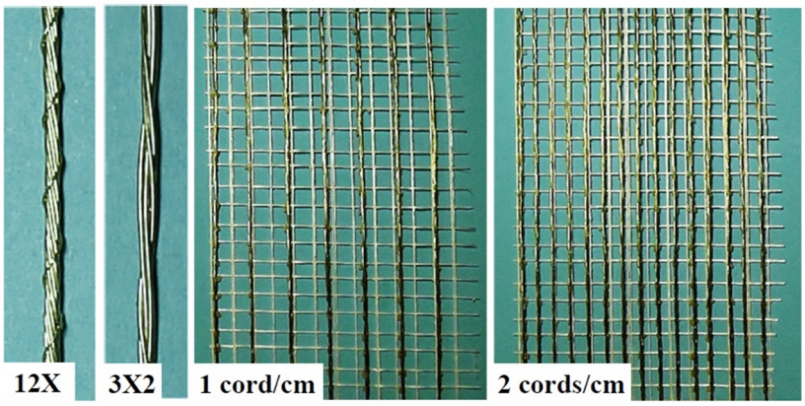

Figure 3: Steel fabric: (a) 12X; (b) 3X2; (c) low density: 1 cord/cm; (d) medium density: 2 cords/cm.

Table 2: Geometrical and mechanical properties of single cord as defined by tests [15].

Fabric type	Cord diameter (mm)	Break (N)	Tensile strength $f_{fu,s}$, MPa	Strain to failure $\varepsilon_{fu,s}$, (mm/mm)	Axial stiffness, $K_{f.s}$ (N/mm): 1 cord/cm	Axial stiffness, $K_{f.s}$ (N/mm): 2 cords/cm
12X	0.889	1160	1870	0.016	8069.3	16138.6
3X2	0.889	1357	2187	0.020		

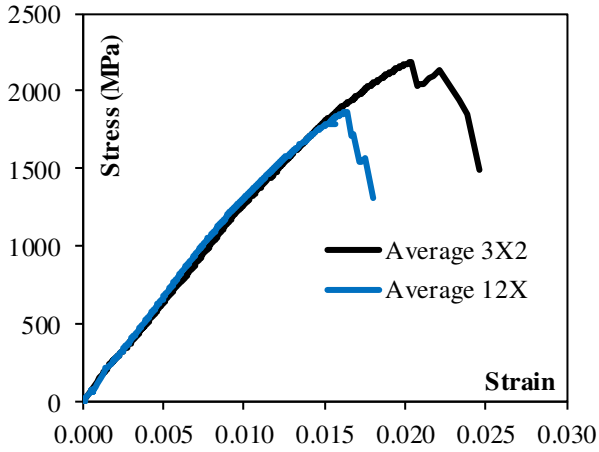

Figure 4: Average stress-strain tensile diagram for the high strength steel cords.

Six specimens (3 from each group) served as control specimens. The rest of the specimens (18 in total) were strengthened with a single-layered SRG jacket with an overlap length that covered three full sides of the specimen [16].

The 24 columns were cast in one batch and tested in two consecutive days. The average compressive strength at the days of the tests was equal to19.4 MPa. The 10 mm diameter ribbed bars had a yield stress of f_{sy}=555 MPa, ultimate stress f_{su}=629 MPa corresponding to StIIIb used in seismic applications in the 1970s. The 6 mm diameter smooth bar reinforcement used for the stirrups had a yield stress of f_{sy}=360 MPa, ultimate stress f_{su}=467 MPa corresponding to StI which was used extensively for shear reinforcement.

The binding material utilized in the SRG jacketing application was a commercial one-component fiber reinforced cementitious grout. The mechanical characteristics at 28 days according to the manufacturer are flexural strength 6.78 MPa, compressive strength 22.1 MPa, adhesion to dry concrete 1.88 MPa and modulus of elasticity 8.03 GPa.

Regarding the notation given to the columns, S and R stand for the square specimens with sharp and rounded edges, respectively. The type of the fabric is defined by its name,12X or 3X2, whereas the terms ℓ and m correspond to the low and medium density fabrics, respectively (ℓ: 1 cord/cm and m: 2 cords/cm). All column tests were performed in triplicate (3 columns for

each type of jacket, Table 1). For example, the R3X2m_2 column corresponds to the second specimen of the square specimens with rounded edges wrapped with the 2 cords/cm 3X2 fabric.

Table 1: Column details.

Notation	Unconfined	Confined	Corner radius (mm)	Fabric/Density code name	Fabric/Density cords/cm	Number of specimens
R	√		25	N/A	N/A	3
R12Xℓ		√	25	12X/low	1 cord/cm	3
R12Xm		√	25	12X/medium	2 cords/cm	3
R3X2ℓ		√	25	3X2/low	1 cord/cm	3
R3X2m		√	25	3X2/medium	2 cords/cm	3
S	√		0	N/A	N/A	3
S12Xℓ		√	0	12X/low	1 cord/cm	3
S3X2ℓ		√	0	3X2/low	1 cord/cm	3
				Total number of specimens:		24

2.2 The SRG jacketing technique

The high strength steel sheets were pre-bent before being applied taking into account the 25 mm corner radius in case of the R-Group columns (Fig. 5(a)). Two pieces of fabric were used along the height of each specimen leaving 1 cm gap between the steel bearing plates of the loading machine and the steel fabric so as to prevent direct axial loading of the jacket. The cementitious grout was applied manually with the help of a trowel directly onto the cleaned and saturated with water lateral surface of the specimens (Fig. 5(b)). The metallic fabric was placed immediately after the application of the cementitious grout (Fig. 5(c)). The grout was squeezed out between the steel fibers by applying pressure manually (Fig. 5(d)-(e)). The bottom jacket was placed first and the upper one followed. One layer of the steel fabric was applied and three full sides of the column were used as an overlap length (Fig. 5(f)). A final coat of the cementitious grout was applied to the exposed surface. The effect on the geometric dimensions of the jacketed specimens was small. The grout layer including the steel reinforced jackets was 7-10 mm thick. The thickness of the grout layer was such as to guarantee that the steel fabric was fully embedded in the cementitious matrix.

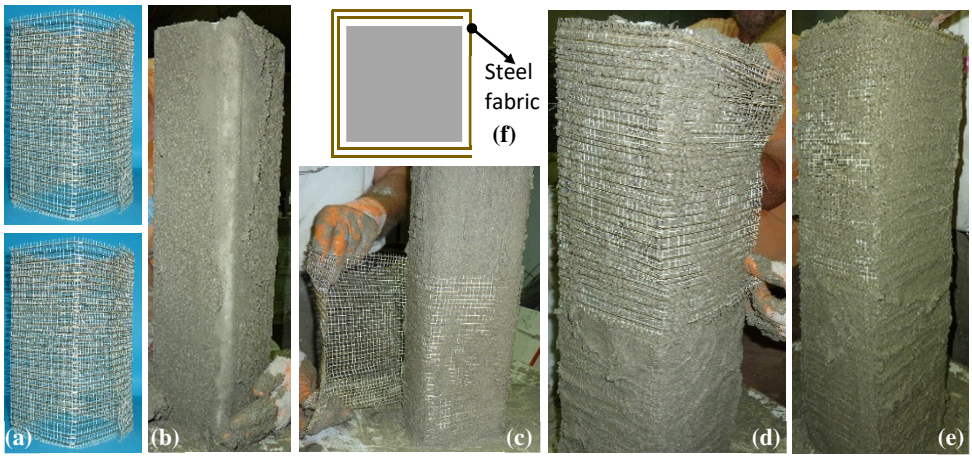

Figure 5: (a) Preparation of the steel fabric; (b) Application of the cementitious grout directly the cleaned and saturated with water lateral surface of the specimen; Application of the (c) bottom jacket and (d) upper layer of the fabric; (e) The specimen after the application of the SRG jacket; (f) Three full sides used as an overlap length.

2.3 Test setup

The specimens were subjected to monotonically increasing concentric uniaxial compression load up to failure. The loading was applied at a rate 0.15 MPa/sec in load control, using a 6000 kN compression testing machine. Axial strain was calculated using the measurements of four linear variable differential transducers (LVDTs) mounted on a top stiff metallic circular plate placed between the load cell and the concrete specimen (Fig. 6(a)). These transducers were placed in the same symmetric way at each one of the four sides for all specimens as shown in Fig. 6(b). The axial load was measured from a load cell placed at the top of the specimen (Fig. 6(a)).

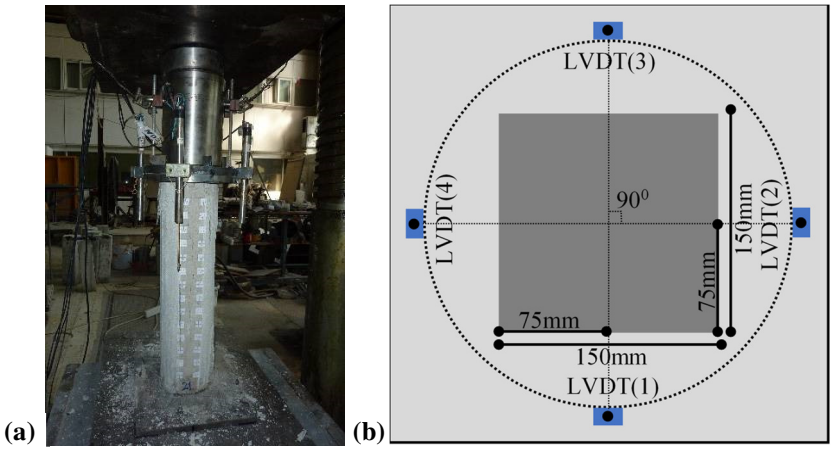

Figure 6: (a) Test setup; (b) Location of LVDTs for axial strain measurements.

3. Test results

3.1 Performance under monotonic axial load

Symmetrical buckling of the longitudinal reinforcing bars either at the top or bottom stirrup spacing was the mode of failure observed in the control specimens owing to the large unsupported length of the bars (Fig. 7, R and S columns).

In general, the SRG confined columns failed due to rupture of the fabric which started from the column corners due to stress concentration. The mode of failure was differentiated to that of debonding for four out of six specimens when the dense fabric of medium density (2 cords/cm) was utilized (Groups R12Xm and R3X2m). The letter (s) has been added at the end of the code-name assigned to these specimens to denote the debonding mode of failure (see Table 3). This debonding mode of failure is believed to have been accelerated by imperfections related to the pre-bending of the fabric to form the steel cage as well as by the small size of the gaps between the steel cords of the dense fabric, a fact that imposed further difficulties in the penetration of the mortar through these gaps [19].

For column cross-sections having larger dimensions than the ones used in the tested specimens the stiffness of the steel jacket will be less prohibiting in forming less imperfect steel jacket than the ones used. This combined with a strict quality control pre-bending of the fabric process could make this influence less significant and improved the final bonding process. An

additional issue is that of the size of the steel jacket mesh. The small opening of the mesh contributes in an increase of the steel cage stiffness. In this way, it results in making the pre-bending process relatively more difficult thus having the detrimental effect in the bonding process that was discussed before. Additionally, the small size of the mesh makes relatively more difficult the penetration of the bonding matrix, thus facilitating the debonding process. These factors should be considered in the construction of this type of jacketing for prototype structural elements when employing steel cages with high axial stiffness.

Failure occurred rather locally by the rupture of the SRG jackets at the sides of the column where only one ply of the fabric was applied. It is pointed out that three full sides of the specimen were used as an overlap length for the steel fabric (Fig. 5(f)). This mode of failure was not influenced by the change in the shape of the cross section.

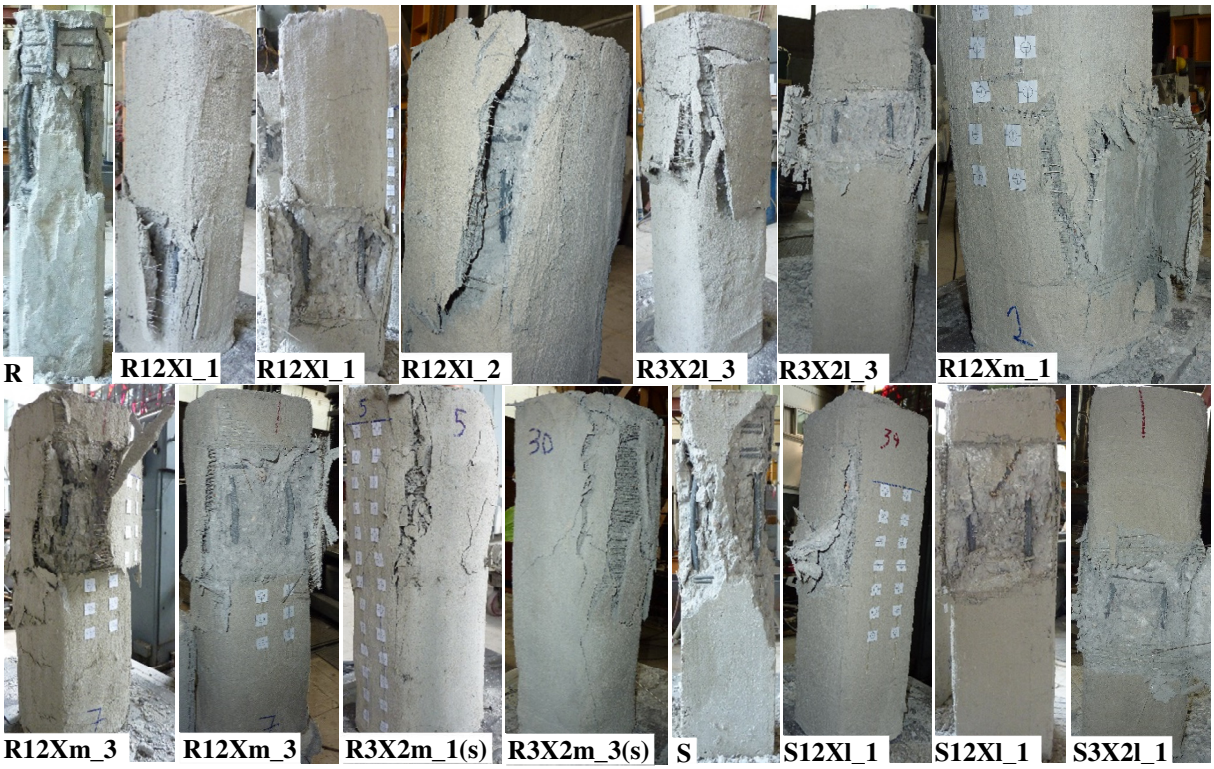

Figure 7: Unconfined and SRG-jacketed RC columns at failure.

Representative SRG confined specimens which failed due to fabric rupture are depicted in Fig. 7. The open stirrups placed at 200 mm distance provided poor support to the longitudinal

reinforcement thus the steel jacket was stretched both by concrete dilation and the outwards buckling of the longitudinal bars. Similar was the mode of failure observed in FRP and TRM confined columns [e.g. 7, 10]. In most of the confined columns, rupture of the fabric occurred at height equal to the stirrup spacing (Fig. 7). Failure occurred gradually since the fracture of the individual steel cords was progressive.

3.2 Strength and strain capacity increase

All the specimens were tested to failure under monotonically increasing concentric compression. The most important mechanical response indices measured during the load tests appear in Table 3. These refer to the peak concrete compressive strength of the confined specimens, f_{cc}, and the corresponding strain, ε_{cc}, to the ultimate compressive strength, $f_{ccu,80\%}$ (corresponds to 20% drop in compressive strength $f_{ccu,80\%} = 0.80 \cdot f_{cc}$) and the corresponding strain, $\varepsilon_{ccu,80\%}$. The compressive strength of the unconfined columns, f_{co}, appears as well.

Table 3 includes values on the jacket confining effectiveness, $K_{c,eff}$, which was calculated as the ratio of the measured peak axial stress sustained by jacketed columns divided by the corresponding measured concrete-core axial strength of the control columns [20]:

$$K_{c,eff} = \frac{\left(f_{cc} - \rho_{\ell} \cdot f_{sy}\right) / \left(1 - \rho_{\ell}\right)}{\left(f_{co} - \rho_{\ell} \cdot f_{s} - \rho_{\text{cov}} \cdot f_{co,o}\right) / \rho_{\text{co}re}}; \quad \rho_{\ell} = \frac{A_{s\ell}}{A_g}; \; \rho_{\text{cov}} = \frac{A_{\text{cov}}}{A_g}; \; \rho_{\text{co}re} = \frac{A_{\text{co}re}}{A_g} \tag{1}$$

where $A_{s\ell}$ is the area of longitudinal reinforcement, A_g is the gross area of the column's cross section, A_{core} the area of the concrete core, A_{cov} the area of the concrete cover, f_{co} and f_{cc} are the concrete compressive strength of the specimens before and after the application of the SRG jackets at the testing period, $f_{co,o}$ is the compressive strength of the unconfined concrete at the testing period, f_{sy} is the yield strength of longitudinal reinforcement and $f_s (\leq f_{sy})$ is the axial stress at the failure axial strain of the control specimens which could be less than the yield strength in case of elastic buckling of the reinforcement.

The measured stress-strain plots for the subgroups of columns of Table 1 appear in Figs. 8(a)-(f). Each graph in these figures includes the axial stress-strain response as derived from the load/displacement measurements for a group of three identical SRG specimens (with their average) and the corresponding unconfined control specimens. For a better insight into the effect of the various employed SRG jacket schemes, the obtained average stress-strain response for either rounded or sharp corners specimens are plotted again in Figs. 9(a) and (b), respectively. Furthermore, in order to focus on the effect of the shape of the cross section (rounded or sharp corners) for the same type of SRG jacket, the relevant average stress-strain response for fabric density 12X/low and 3X2/low is plotted again in Fig. 9(c) for comparison.

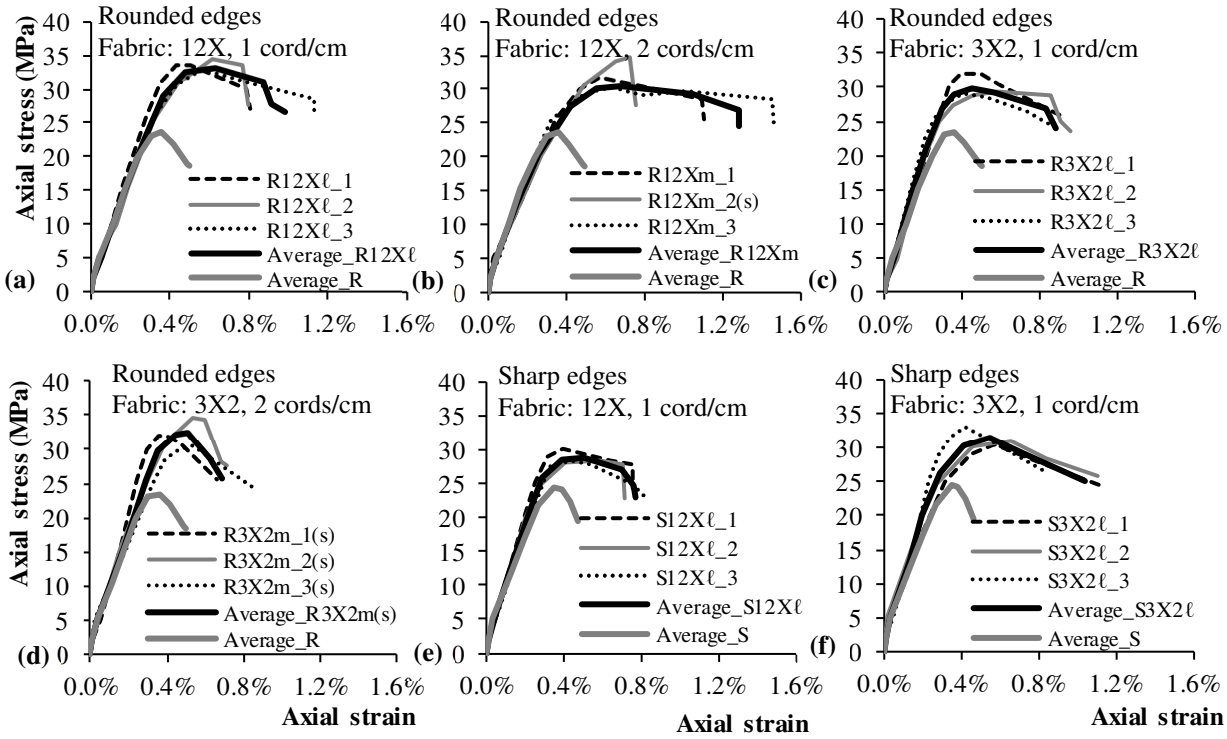

Figure 8: Axial stress – strain curves of the tested columns.

In general, the application of a single layer of SRG jacket proved to be efficient in increasing both the strength (by 19% to 43%, Table 3) and the strain capacity (by 281% and 544%, Table 3). Strength and strain increase are defined as $(f_{cc}-f_{co})/f_{co}$ and $(\varepsilon_{ccu}-\varepsilon_{co})/\varepsilon_{co}$, respectively, with ε_{co}=2‰. Moreover, the SRG jackets resulted in delaying buckling of the longitudinal

reinforcement. The application of single-layered SRG jackets with the 1 and 2 cords/cm 12X and 3X2 fabrics to the specimens with rounded edges resulted in almost 100% increase of the confining effectiveness compared to the corresponding unconfined specimens ($K_{c,eff}$ ranged between 1.91 and 2.22, see Table 3). $K_{c,eff}$ was lower for the SRG specimens with sharp edges (1.57 and 1.75 for the 12X and 3X2 single-layered SRG jackets, respectively, see Table 3).

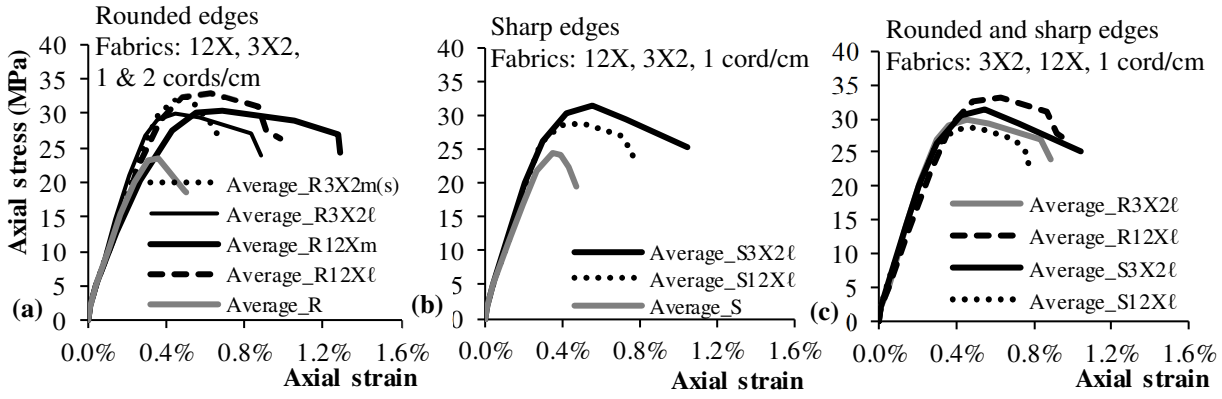

Figure 9: Average axial stress – strain curves of the tested columns.

As can be seen in Fig. 9(a) for the specimens with rounded edges, the 1 cord/cm density SRG jackets resulted in strength increase corresponding to 43% and 28% for the R12Xℓ and R3X2ℓ sub-groups of columns, respectively, (Table 3). In case of the specimens with sharp edges where the same density fabric was utilized, the average compressive strength increase is 19% and 29% for the S12Xℓ and S3X2ℓ specimens, respectively (Fig. 9(b)). Although the 3X2 fabric has a higher tensile strength compared to the 12X fabric (17% higher as seen in Table 2), the R3X2ℓ columns did not exhibit higher compressive strength when compared to the R12Xℓ columns. The opposite was observed for the specimens with the sharp edges where the S3X2ℓ columns resulted in 8.2% higher average compressive strength when compared to the S12Xℓ columns. This observation highlights the importance of the quality of bond developed between the fabric and the mortar which is in direct relationship to the construction details of the SRG jacketing system discussed in Section 3.1.

By comparing the increase in the average compressive strength achieved by employing the 1 cord/cm fabric as compared to the strength achieved by employing the 2 cords/cm fabric the following observations can be made:

i) Employing the 1 cord/cm 12X fabric jacket (i.e. R12Xℓ specimens) the average compressive strength increase is 43% whereas employing the denser (2 cords/cm) 12X fabric jacket (i.e. R3X2m specimens) the corresponding increase is 32%. Thus, for this type of fabric the increase of fabric density did not result in a further average compressive strength increase. Furthermore, it can also be observed, that for specimen R12Xm_2(s) which exhibited a larger than the average strength increase this was accompanied by the debonding mode of failure. It is interesting to note that the other two specimens of this group (R12Xm) developed fracture of the SRG jacket for strength values smaller than the corresponding value of specimen R12Xm_2(s).

ii) Employing the 1 cord/cm 3X2 fabric jacket (i.e. R3X2ℓ specimens) the average compressive strength increase is 28% whereas employing the denser (2 cords/cm) 3X2 fabric jacket (i.e. R3X2m specimens) the corresponding increase is 38%. Thus, for this type of fabric the increase of fabric density resulted, as expected, in a modest average compressive strength increase. However, this increase was accompanied in all specimens of this group (R3X2m) with the debonding mode of failure.

Both these observations lead to the conclusion that the increase in the fabric density for the studied SRG jackets does not necessarily lead to an increase in the compressive strength. This can be partly explained by the triggering of the debonding mode of failure, which was discussed in Section 3.1 and was attributed to the imperfections related to the pre-bending of the denser fabric jackets as well as the bond mechanism between the used matrix and the fabric, being also affected by the size of the gaps. Therefore, for this type of SRG jacketing the increase in the compressive strength is not controlled by the density of the fabric but rather from the quality

and effectiveness of the bond between the cords of the fabric and the used inorganic matrix together with all the construction details during the application of this jacketing.

When studying the effect of the cross-section shape (either with rounded or sharp edges) on the measured average compressive strength (Table 3, Fig. 9(c)) the following observations can be made. By comparing specimens R12Xℓ with S12Xℓ it is seen that the sharp edges for this type of SRG jacket lead to a 13.6% average compressive strength decrease. On the contrary, by comparing specimens R3X2ℓ with S3X2ℓ it is seen that the sharp edges specimens confined with this type of SRG jacket exhibited an average compressive strength 4.7% higher than the specimens with rounded edges. The use of the steel reinforced fabrics due to their lower axial stiffness compared to that of the composite fabrics used in FRP jacketing results in rather low stress concentration in the region of relatively sharp corners thus sustaining the effectiveness of the confinement as the corner radius decreases. Additionally, the use of the cementitious matrix provides stress smearing action at the corners. Further research is necessary to verify the effect of the sharp corner on the increase of the compressive strength by SRG jacketing.

The plastic strain range of the confined specimens, when compared with the unconfined control specimens, increased by 357%, when using the 1 cord/cm 12X and 3X2 fabrics, and by 544% when using the 2 cords/cm 12X fabrics (the R3X2m specimens were not considered due to the debonding mode of failure). The strain increase for the SRG confined columns with the sharp corner cross section shape is within the range of the values reported for the rounded corner cross section columns (281% and 412% for the 12X and 3X2 fabric jackets, respectively, Table 3). It seems that the 12X fabric jackets applied to square cross section columns led to the most unfavourable response (Fig. 9b).

The strain ductility ratios were calculated for those SRG jacketed columns that failed in rupture as to further assess the confinement effectiveness of the applied SRG jacketing schemes (Table 3). The strain ductility ratio, μ_ε, is defined as the ultimate strain, ε_u, divided by the yield

strain, ε_y (Fig. 10). The stress – strain curve was converted to a bilinear curve considering that the linear branch of the bilinear curve intersected the experimental curve at 60% of the yield stress and that the ultimate strain corresponds to a 20% drop from the peak load [16]. The area below the bilinear curve is equal to the area below of the experimental curve. In cases where a post-peak branch does not exist, the ultimate strain is defined by the last strain measurement in the stress-strain curve.

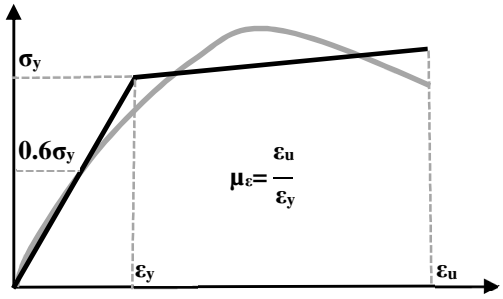

Figure 10: Bilinearization of the stress – strain response curve for strain ductility definition.

The use of the 2 cords/cm 12X fabric in the rounded corner columns provided 42% higher strain ductility ratios when compared to the lower density 12X fabric (μ_ε=3.57 vs 2.52 for R12Xm and R12Xℓ, respectively, Table 3). In the same group of columns, wrapping with the low density 3X2 fabric managed to increase ductility to the same levels as the denser 12X fabric. The comparison between the average values of the strain ductility ratios for the same type of SRG jackets when applied to sharp and rounded corner columns indicates that the sharp corner columns presented a marginally higher ductility increase. This was also observed in Reference [16].

Table 3: Test results of R- and S-Group of columns.

Column notation (mode of failure)	Compressive strength, f_{cc} (MPa)		Ultimate compr. strength, $f_{ccu,80\%}$ (MPa)		Strain, ε_{cc}		Ultimate strain, $\varepsilon_{ccu,80\%}$		$K_{c,eff}$	f_{cc}/f_{co}	$\varepsilon_{ccu,80\%}/\varepsilon_{co}$#	Strain ductility, μ_ε	
	value	Mean/SDV	value	mean	value	mean	value	mean				value	mean
R_1	26.9		21.5		0.00343		0.00450					1.61	
R_2	22.9	23.5 / 3.1	18.3	18.8	0.00395	0.00360	0.00502	0.00483	1.00	1.00	1.00	2.20	2.08
R_3	20.8		16.7		0.00342		0.00497					2.43	
R12Xℓ _1 (rupture)	33.7		26.9		0.00505		0.00807					2.46	
R12Xℓ _2 (rupture)	34.4	33.7 / 0.56	27.5	26.9	0.00616	0.00563	0.00800	0.00914	2.22	1.43	4.57	1.95	2.52
R12Xℓ _3 (rupture)	33.0		26.4		0.00567		0.01135					3.15	
R12Xm_1 (rupture)	31.9		25.5	25.8	0.00577	0.00646	0.01108					2.73	
R12Xm_2(s) (debonding)	34.7	32.2/2.27	27.7		0.00724		0.00754	0.01110	2.10			-	3.57
R12Xm_3 (rupture)	30.2	31.0$/1.2$	24.2	24.8$	0.00638	0.00608$	0.01467	0.01288$	1.99$	1.32$	6.44	4.41	
R3X2ℓ _1 (rupture)	32.0		25.6		0.00497		0.00905					2.89	
R3X2ℓ _2 (rupture)	29.3	30.1 / 1.65	23.4	24.4	0.00580	0.00493	0.00965	0.00916	1.91	1.28	4.58	3.34	3.29
R3X2ℓ _3 (rupture)	29.0		24.1		0.00401		0.00880					3.63	
R3X2m_1(s) (debonding)	32.0		25.6		0.00352		0.00659					-	
R3X2m_2(s) (debonding)	34.7	32.4 / 2.13	27.7	25.9	0.00530		0.00714	0.00740	2.11	1.38	3.70	-	-
R3X2m_3(s) (debonding)	30.5		24.4		0.00531	0.00471	0.00849					-	
S_1	24.1		19.3		0.00418		0.00444					1.85	
S_2	25.4	24.4 / 0.81	20.3	19.6	0.00355	0.00356	0.00522	0.00459	1.00	1.00	1.00	2.00	1.86
S_3	23.9		19.1		0.00296		0.00409					1.73	
S12Xℓ_1 (rupture)	30.2		24.1		0.00395		0.00759					2.71	
S12Xℓ _2 (rupture)	28.5	29.1 / 0.98	22.8	23.3	0.00589	0.00475	0.00711	0.00761	1.57	1.19	3.81	2.65	2.70
S12Xℓ _3 (rupture)	28.5		22.8		0.00442		0.00815					2.75	
S3X2ℓ _1 (rupture)	30.4		24.3		0.00572		0.01123					3.79	
S3X2ℓ _2 (rupture)	31.0	31.5 / 1.42	24.8	25.2	0.00650	0.00549	0.01110	0.01024	1.75	1.29	5.12	4.17	3.62
S3X2ℓ _3 (rupture)	33.1		26.4		0.00424		0.00840					2.90	

A common value for ε_{co} equal to 2 ‰ is considered in order for the $\varepsilon_{ccu,80\%}$ values of columns to be compared, $ average from R12Xm_1, R12Xm_3.
The symbol (s) signifies the columns that failed due to debonding of the SRG jacket. The rupture mode of failure signifies the fracture of parts of the SRG jacket.

4. Analysis of the test results

4.1 Confining pressure exerted by the SRG jacket

Similar to the FRP jacketing [20, 21], the average confining pressure exerted by the SRG jacketing system when applied to RC members is obtained as the average lateral stress developing in the two principal directions of the cross section as:

$$\sigma_{lat,ave} = \frac{1}{2}\underbrace{\left(\sigma_{lat,x}^{SRG} + \sigma_{lat,y}^{SRG}\right)}_{SRG\ \text{confinement}} + \frac{1}{2}\underbrace{\left(\sigma_{lat,x}^{st} + \sigma_{lat,y}^{st}\right)}_{stirrup\ \text{confinement}} = \frac{1}{2}\left(\underbrace{\alpha^{SRG}\cdot\rho_v^{SRG}\cdot E_f\cdot\varepsilon_{s,eff}}_{SRG\ \text{confinement}} + \underbrace{\alpha^{st}\cdot\rho_v^{st}\cdot f_y^{st}}_{stirrup\ \text{confinement}}\right) \quad (2)$$

where E_f is the modulus of elasticity of the SRG jacket and $\varepsilon_{s,eff}$ is the effective tensile strain that develops in the jacket near failure which may occur either by debonding or rupture, whichever prevails [21]. The steel fabric is considered to have an equivalent thickness, t_{eq}, per unit width [15]. The first and second part of Eq. (2) correspond to the contribution of the SRG jacket and stirrups, respectively. The subscripts x and y denote transverse pressure in the two principal directions of the cross section. $\rho_v^{SRG}(=2t_{eq}(b+d)/(bd))$ is the volumetric ratio of the SRG reinforcement and ρ_v^{st} the volumetric ratio of stirrups. The terms α^{SRG} and α^{st} are the confinement effectiveness factors for the SRG jacket and stirrup contribution, respectively. The term $\alpha^{st}(=\alpha_n\cdot\alpha_s)$ defined according to EC8-Part I [22] was estimated equal to 0.013 for the ∅6/200 stirrups. The low value of α^{st} indicates the negligible confinement effect of small bar diameter placed at sparse stirrup arrangement. The a^{SRG} is defined as [23] (Fig. 11):

$$\alpha^{SRG} = 1 - \frac{(b-2r)^2 + (h-2r)^2}{3A_g(1-\rho_l)} \quad (3)$$

where b, h are the width and height of the cross section, r is the corner radius, A_g is the cross sectional area and ρ_l is the percentage of the longitudinal reinforcement. The square columns with rounded edges (r=25 mm) had α^{SRG}=0.70, whereas in the square columns with the sharp edges (r=0) only one third of the cross section is well-confined (i.e. α^{SRG}=0.32).

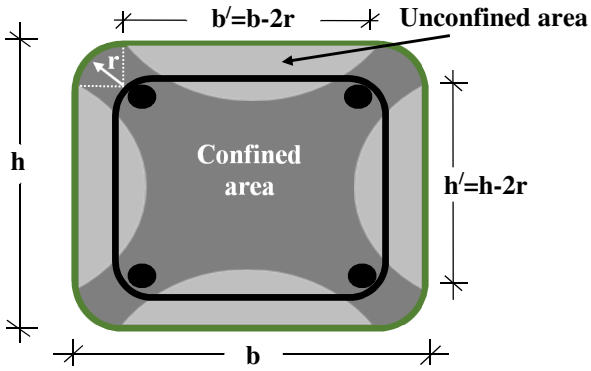

Figure 11: Confined and unconfined regions in SRG confined rectangular RC cross section

For a better understanding of the effect of the various jacketing systems tested herein, the lateral confining pressure, σ_{lat}, is normalized to the compressive strength of the unconfined concrete, $f_{co,o}$ (=19.4 MPa). Three levels of confinement are identified corresponding to the low density 12X and 3X2 (i.e. 1 cord/cm) SRG jacketed specimens with sharp edges ($\sigma_{lat}/f_{co,o}$=0.03), the low and medium (i.e. 2 cords/cm) density 12X and 3X2 SRG jacketed specimens with rounded edges (low density jackets: $\sigma_{lat}/f_{co,o}$=0.06 and medium density jackets $\sigma_{lat}/f_{co,o}$=0.11). The average values of the normalized lateral confining pressure, $\sigma_{lat}/f_{co,o}$, are plotted again the corresponding average values of the normalized experimental compressive strength, $(f_{cc}/f_{co,o})^{exp}$, and the experimental values of the axial strain at 20% post-peak strength loss, $\varepsilon_{ccu,80\%}$, in Figs. 12(a) and (b), respectively.

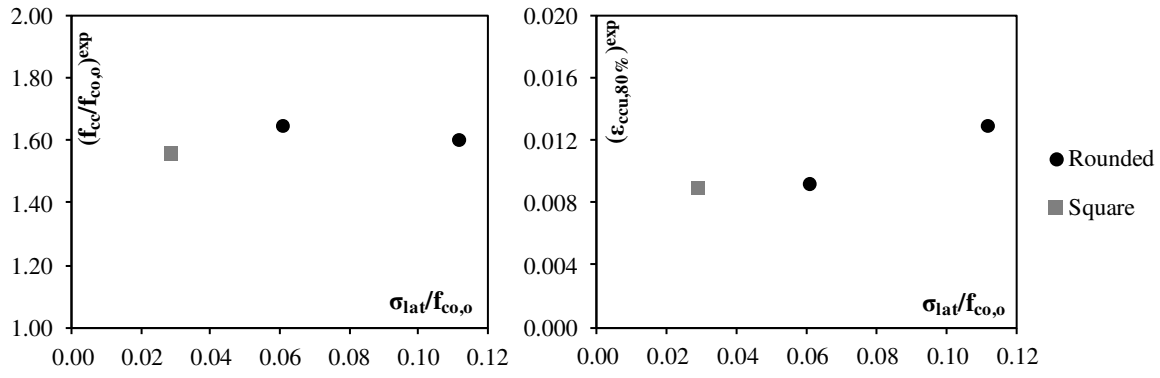

Figure 12: (a) $(f_{cc}/f_{co})^{exp}$ versus (σ_{lat}/f_{co}) and (b) $\varepsilon_{ccu,80\%}$ versus (σ_{lat}/f_{co}) for the columns that failed due to rupture.

As is shown in Fig. 12(a), the difference in strength increase expressed by $(f_{cc}/f_{co,o})^{exp}$ between the alternative jacketing schemes is marginal. Thus, in case of the low density fabrics (1 cord/cm) the specimens with the sharp edges resulted in 5.5% lower strength compared to the specimens with rounded edges. Moreover, the medium density (2 cords/cm) SRG jackets when applied to the square columns with rounded edges seem to be equally effective with the low density ones. This is related to the quality of the bond developed between the medium strength steel cords when immersed in the inorganic matrix as discussed above. The results related to $\varepsilon_{ccu,80\%}$ indicate a marginal difference between the square columns with rounded and sharp edges. The $\varepsilon_{ccu,80\%}$ reached by 40% higher value in case of the medium density fabric (2 cords/cm). The observations related to the medium density fabric should be seen with caution due to the small number of RC columns tested.

From the preceding discussion, it is evident that the low axial stiffness of the 1 cord/cm SRG systems used in this study results in rather low stress concentration in the region of relatively sharp corners thus sustaining the effectiveness of the confinement as the corner radius decreases. Furthermore, the use of the cementitious matrix provides stress smearing action at the corners. This observation is in accordance with the findings of a previous study related to influence of the cross section shape on the behavior of SRG-confined prismatic concrete members [16].

4.2 Effectiveness of the SRG system in delaying buckling of the longitudinal steel bars

In the present experimental investigation, the application of SRG jackets to RC columns with sparsely spaced stirrups managed to delay but not to preclude buckling of compression reinforcement. According to the mechanics of longitudinal bars embedded in concrete prismatic members, when the bar reaches critical conditions (i.e. instability), it bends laterally to maintain compatibility with the increasing axial strain of the supporting concrete core [3]. Therefore, the concrete core becomes overstressed and crushing occurs. The critical axial compression

concrete strain of the SRG confined columns is in direct relationship with the mobilized lateral confining pressure. At the same time, the longitudinal bar buckles symmetrically at a stress $f_{s,crit}$ which is related to the available s/D_b ratio [10, 20, 24, 25]:

$$\frac{s}{D_b} = 1.5\sqrt{\frac{E_i}{f_{s,crit}}} \tag{4}$$

where s is the stirrups spacing (unsupported length) and D_b is the bar diameter of the longitudinal reinforcement. E_i could be either the tangent modulus of steel at the stress level considered, E_h [24], or the double modulus of elasticity, E_r [25], defined as (Fig. 13(a)):

$$E_{hi} = p\left(\frac{f_u - f_y}{\varepsilon_u - \varepsilon_y}\right)\left(\frac{\varepsilon_u - \varepsilon_{s,crit}}{\varepsilon_u - \varepsilon_h}\right)^{p-1} \;;\; p = E_{ho}\frac{\varepsilon_u - \varepsilon_h}{f_u - f_y} \tag{5a}$$

$$E_r = \frac{4 \cdot E_s \cdot E_{sec}}{\left(\sqrt{E_s} + \sqrt{E_{sec}}\right)^2} \tag{5b}$$

The strain values at yielding, at the end of the yielding plateau and ultimate, ε_y, ε_h and ε_u, along with the stress values at yielding and ultimate, f_y and f_u, for the longitudinal reinforcement used in this study appear in Fig. 13(a). The term $\varepsilon_{s,crit}$ corresponds to the axial strain at which the bar becomes unstable.

The compressive strain ductility, $\mu_{\varepsilon s}$, is plotted against the s/D_b ratio for the stress-strain law of the longitudinal bars used in the tests following the two different definitions of the modulus of elasticity in Fig. 13(b) (For more details, see the References [10, 20, 21]). The critical buckling strain, $\varepsilon_{s,crit}$, for much lower s/D_b ratios (roughly equal to 7 and 11 depending on the definition of the elastic modulus, E_i) than the one used in the experiments corresponds to two times the yielding strain of steel (i.e. strain at the end of the yielding plateau) ($\mu_{\varepsilon s,crit}$=2, Fig. 13(b)).

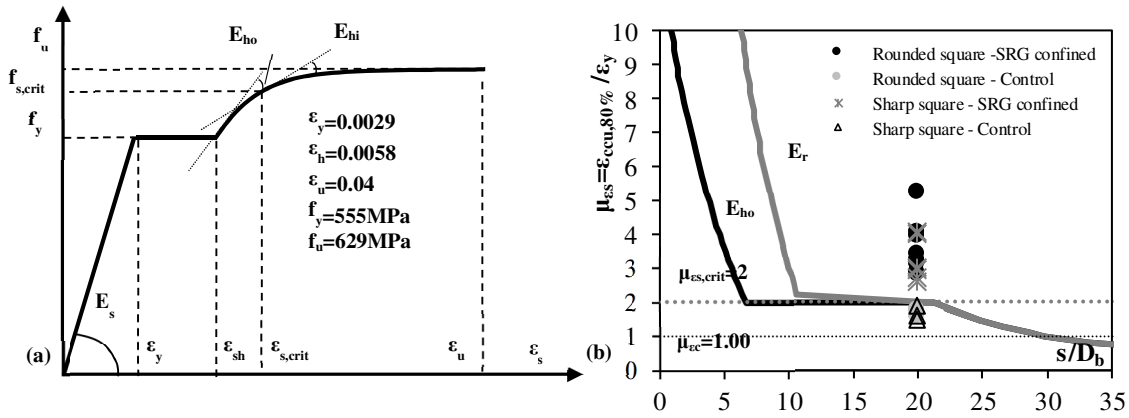

Figure 13: (a) Stress – strain diagram and (b) Compressive strain ductility, $\mu_{\varepsilon c}$, versus stirrup spacing s/D_b for the longitudinal reinforcement used in the tests.

The experimental values of the compressive strain ductility, $\mu_{\varepsilon c}$, for the control and the SRG jacketed column specimens corresponding to $s/D_b=20$ that failed due to rupture of the fabric appear in Fig. 13(b). The control columns failed with an average value of $\mu_{\varepsilon c}$ equal to 1.64 and 1.73 for the sharp and rounded corner columns, respectively (see Fig. 13(b)). It seems that the longitudinal reinforcement just after yielding could not carry any further load, resulting thus to concrete core overload which led to instant failure.

SRG confinement increased the $\mu_{\varepsilon c}$ values attained by the substandard RC columns to values ranging from 2.55 to 4.03 and from 2.84 and 5.26 for the SRG confined columns with sharp and rounded corner edges, respectively (Fig. 13(b)). The SRG jackets prohibited the premature instability of the longitudinal reinforcing bars and postponed the occurrence of their buckling at higher strain levels thus resulting to an increased compressive strength capacity of the concrete core. Rupture of the steel fabric occurred immediately upon the longitudinal reinforcement became unstable owing to the localized stress concentrations in the mid-distance between successive stirrups.

5. Conclusions

An experimental investigation was carried out in order to study the efficiency of SRG jackets in delaying bar buckling in substandard RC columns subjected to uniaxial compression. Single-layered SRG jackets were applied to 18 out of the 24 RC columns designed to be susceptible to premature buckling. The shape of the cross section was square with either sharp or rounded edges. The alternative jacket schemes were differentiated as to the density of the fabric (1 and 2 cords/cm) and type of cords (12X and 3X2). The following conclusions are drawn:

a) All columns failed due to bar buckling independently of the shape of the cross section. Rupture of the fabric was the dominant mode of failure of the specimens with the low density fabric (1 cord/cm), which occurred at height equal to the stirrup spacing with progressive fracture of the individual steel cords. The debonding mode of failure was observed in the majority of the medium density (2 cords/cm) SRG jackets mainly due to imperfections related to the pre-bending of the fabric to form the steel cage as well as to difficulties in the penetration of the mortar through the small size of the gaps between the steel cords. These factors should be considered in the construction of this type of jacketing for prototype structural elements when employing steel cages with high axial stiffness.

b) Confinement of RC columns having sparse transverse reinforcement (s/D_b=20) with single-layered SRG increased compressive strength and deformation capacity from 19% to 43% and from 270% to 544%, respectively. The average strain ductility was increased from 2.5 to 3.6.

c) The comparison between the average values of the strain ductility ratios for the same type of SRG jackets when applied to sharp and rounded corner columns indicated that the sharp corner columns presented a marginally higher ductility increase.

d) It was shown that in case of steel fabrics with low axial stiffness, the effectiveness of the SRG confinement is smaller for sharp specimens than for specimens with rounded edges.

However, the effect of the sharp or rounded edges on the increase of the compressive strength by SRG jacketing needs further research.

e) The increase in the fabric density for the studied SRG jackets does not lead to an increase in the compressive strength. This can be partly explained by the triggering of the debonding mode of failure. For this type of SRG jacketing the increase in the compressive strength is not controlled by the density of the fabric but rather from the quality and effectiveness of the bond between the chords of the fabric and the used inorganic matrix together with all the construction details during the application of this jacketing.

f) The application of SRG jackets to RC columns with sparsely spaced stirrups managed to delay but not to preclude buckling of compression reinforcement. The compressive strain ductility increases from 2.6 to 5.3.

g) The SRG jacketing is a promising confinement technique that can modify the response of old-type RC columns with substandard detailing from one of low ductility to one of moderate ductility. Further research should focus on the effect of multiple layers of different density in conjunction with the examination of a range of geometric and material properties of the SRG jackets.

Acknowledgements

The program was conducted in the Laboratory of Strength of Materials and Structures, Civil Engineering Department, Aristotle University of Thessaloniki. The authors wish to thank Mr. T. Koukouftopoulos for his assistance in the experimental program. Many thanks to Professor S.J. Pantazopoulou, Civil Engineering Department, Lassonde Faculty of Engineering, York University (Canada) and Assistant Professor S. Tastani, Civil Engineering Department, Demokritus University of Thrace (Greece) for their help in deriving the $\mu_{\varepsilon c}$ - s/D_b, curves for the longitudinal reinforcement used in the tests. The materials were donated by SIKA and Interbeton. The first author wish to acknowledge the financial support provided by the European

Union's Horizon 2020 research and innovation programme under the Marie Skłodowska-Curie grant agreement No 700863.

References

[1]. Mau, S. Effect of tie spacing on inelastic buckling of reinforcing bars. ACI Structural Journal, 1990;87(6):671-677.

[2]. Monti G, Nuti C. Nonlinear cyclic behavior of reinforcing bars including buckling. J Struct Eng 1992;118(12):3268-3284.

[3]. Pantazopoulou S. Detailing for reinforcement stability in RC members. J Struct Eng 1998;124(6):623-632.

[4]. Yalcin C, Saatcioglu M. Inelastic analysis of reinforced concrete columns. Comp Struct 2000;77:539-555.

[5]. Maalej M, Tanwongsval S, Paramasivam P. Modelling of rectangular RC columns strengthened with FRP. Cem Concr Comp 2003;25(2):263-276.

[6]. Pantazopoulou SJ, Tastani SP, Thermou GE, Triantafillou T, Monti G, Bournas D Guadagnini M. Background to European seismic design provisions for the retrofit of R.C. elements using FRP materials. Fib Struct Concr J 2016;17(2):133–305.

[7]. Bournas DA, Lontou PV, Papanicolaou CG, Triantafillou TC. Textile-Reinforced Mortar versus Fiber-Reinforced Polymer Confinement in Reinforced Concrete Columns. ACI Struct J 2007;104(6):740-748.

[8]. Manos GC, Kourtides V. Retrofitting of long rectangular R/C cross-sections with partial confinement employing carbon fiber reinforcing plastics. Greece, Patras: FRPRCS-8 Conf 2007; Paper No. 128.

[9]. Manos GC, Katakalos K. The use of fiber reinforced plastic for the repair and strengthening of existing reinforced concrete structural elements damaged by earthquakes. In: Masuelli MA, editor. Fiber reinforced polymers - The technology applied for concrete repair: 2013; ISBN 978-953-51-0938-9.

[10]. Tastani S, Pantazopoulou S, Zdoumba D, Plakantaras V, Akritidis E. Limitations of FRP jacketing in confining old-type reinforced concrete members in axial compression. J Compos Constr 2006;10(1):13-25.

[11]. Thermou GE, and Pantazopoulou SJ. Fiber reinforced polymer retrofitting of substandard RC prismatic members. J Compos Constr 2009;13(6):535-546.

[12]. Bournas DA, and Triantafillou TC. Bar buckling in rc columns confined with composite materials. J Compos Constr 2011; 15(3):393-403.

[13]. Thermou GE, Pantazopoulou SJ. Metallic fabric jackets: an innovative method for seismic retrofitting of substandard RC prismatic members. Fib Struct Concr J 2007;8(1):35-46.

[14]. Thermou GE, Katakalos K, and Manos G. Influence of the loading rate on the axial compressive behavior of concrete specimens confined with SRG jackets. Greece, Kos: ECCOMAS Thematic Conference COMPDYN 2013; Paper No. 1482.

[15]. Thermou GE, Katakalos K and Manos G. Concrete confinement with steel-reinforced grout jackets. Mater Struct 2015;48(5):1355-1376.

[16]. Thermou GE, Katakalos K, Manos G. Influence of the cross section shape on the behaviour of SRG-confined prismatic concrete specimens. Mater Struct 2016;49(3):869-887.

[17]. El-Hacha R, Abdelrahman K. Slenderness effect of circular concrete specimens confined with SFRP sheets. J Compos B Eng 2013;44(1):152–166.

[18]. Lam L, Teng JG. Stress-strain model for FRP-confined concrete under cyclic axial compression. Eng Struct 2009;31(2):308-321.

[19]. Papakonstantinou CG, Katakalos K. Flexural behavior of reinforced concrete beams strengthened with a hybrid retrofit system - Steel fiber retrofit system. Struct Eng Mech 2009;31(5):567-585.

[20]. Tastani S, Pantazopoulou, S. Experimental evaluation of FRP jackets in upgrading RC corroded columns with substandard detailing. Eng Struct, 2004;26(6):817–829.

[21]. Tastani S, Pantazopoulou S. Detailing procedures for seismic rehabilitation of reinforced concrete members with fiber reinforced polymers. Eng Struct 2008;30(2):450-461.

[22]. Eurocode 8, Design of structures for earthquake resistance - Part I: General Rules, seismic actions and rules for buildings, EN1998-1-2004: E, European Committee for Standardization (CEN), Brussels, 2004.

[23]. fib Bulletin 14, Externally Bonded FRP Reinforcement for R.C. Structures. Report by Task Group 9.3, federation international du béton (fib), Lausanne Switzerland, 2001.

[24]. Priestley M, Seible F, Calvi M. Seismic design and retrofit of bridges, Wiley, New York, 1996.

[25]. Papia M, Russo G, Zingone G. Instability of longitudinal bars in RC columns. J. Struct. Eng 1988;114(2):445–461.